SF2A 2024
M. Béthermin, K. Baillié, N. Lagarde, J. Malzac, R.-M. Ouazzani, J. Richard, O. Venot, A. Siebert (eds)

CHARACTERIZATION OF THE PROPERTIES OF EXTENDED UV REGIONS IN NEARBY GALAXIES WITH DEEP LARGE OPTICAL SURVEY

E. Bernaud[1], S. Boissier[1], Junais[2] and E. Hugot[1]

Abstract. The new large deep optical survey (like those performed with MegaCam at CFHT, DES, LSST, Euclid) bring the promise to better study Low Surface Brightness Galaxies (LSBs). A new telescope suitable for observing LSBs, CASTLE, is under construction at LAM in Marseille to test innovative concepts (curved detector, reduction in the number of optics, removal of supporting spiders and associated diffraction effects). One of the science cases proposed for this telescope (Lombardo et al. 2020) is the characterization of the optical part of the extended UV (XUV) galaxies discovered by GALEX (Thilker et al. 2007). Very large and faint galaxies discovered instead in the optical domain have been called "Giant LSBs" (e.g. Sprayberry et al. 1995) based on the diffuseness of their extended disk. Through a systematic optical study of the disks of XUV galaxies, we will be able to determine the tentative relationship between XUV and LSBs galaxies. We selected several XUV galaxies for which deep optical data are already available from the deep DES survey and compared them with the UV data from GALEX. We present a preliminary analysis for the first three galaxies studied and show that it is possible to perform such a study with DES data. The first results indicates a diversity of cases in the Giant LSB vs XUV galaxies connection.

Keywords: galaxies, low surface brightness, extended-UV galaxies

1 Introduction

The discovery of eXtended-UV Galaxies (XUV) questioned our understanding of galaxies (Thilker et al. 2007). Those galaxies are characterized by an UV emission in an extended disk beyond the R_{25} (the radius corresponding to a radially averaged surface brightness of 25 mag arcsec^{-2} in B-Band) and classified in two different types. Type one represents XUV galaxies with structured ultra violet emission beyond the R_{25} while the type two is defined by a large blue LSB zone in the optical. Boissier et al. (2008) and Hagen et al. (2016) discussed the possibility of a link between XUV and Giant Low Surface Brightness galaxies (GLSB), galaxies characterized by a disk of large luminosity, but low surface brightness due to their large radial extent (Sprayberry et al. 1995). According to the classification of Thilker et al. (2007), Malin 1, the largest and most iconic among GLSBs is also a XUV galaxies (Boissier et al. 2008). Hagen et al. (2016) showed that UGC1382 is both XUV and LSB. This connection between the two type of extended galaxies bring up questions about origins, characteristics and evolution on those galaxies. Could XUV and GLSB galaxies be related? Are they the same galaxies with a different selection (XUV being selected in the UV while GLSB are defined from the optical), or two distinct families? Do they share common properties? We propose to investigate those questions by studying XUV galaxies for which deep optical images are available.

2 Analyse

Sprayberry et al. (1995) proposed to define GLSB on the basis of a figure separating LSB (regular Low Surface Brightness galaxies, that may be dwarfs), GLSB, and normal galaxies. This figure compares the central surface brightness in the B-Band, $\mu_B(0)$, with the scale length of the disk component of the galaxies (R_s in kpc). The separation between GLSB and LSB is the function $\mu_B(0) + 5log(R_s) = 27$ represented by the blue line in Fig.1.

[1] Aix Marseille Univ, CNRS, CNES, LAM, Marseille, France
[2] NCBJ, Warsow, Poland

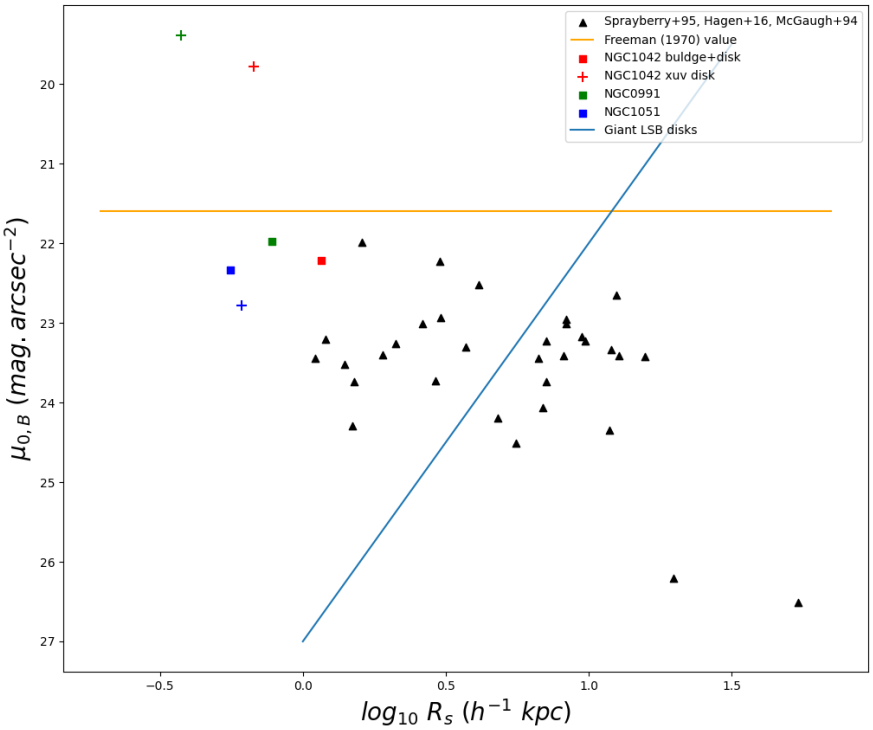

Fig. 1. Classification of the sample adapted from Sprayberry et al. (1995). The squares symbols represent the value of the disk fit for the inner part of the galaxies and the cross symbols for the extended UV region. The blue line distinguishes the LSB galaxies from Giant LSB (GLSB) galaxies. The orange line, the Freeman (1970) value (21.65 $mag/arcsec^2$), separates the high surface brightness (HSB) galaxies from the LSB galaxies.

As a first step of comparing GLSBs and XUVs, we propose to add the XUV galaxies in this figure, in order to identify potential relationships between XUV galaxies and GLSB galaxies. To achieve this, we have performed an exponential fit of the surface brightness profiles in each galaxy in our sample, with one fit derived for the inner region (from the center to R_{25}) and the other for the "XUV region". This XUV region spans from R_{25} to the UV radius (R_{UV}) for which we propose a definition in the next section. The sample of this study is composed of nine XUV galaxies from Thilker et al. (2007) and for which DES (Abbott et al. 2021) data are available. In this publication, we focus on three of them: NGC1042, NGC991 and NGC1051, the first one being studied on the basis of various data set in the literature, allowing us to compare our method and results with others.

2.1 Method

We obtain surface brightness profiles following the steps described below. We start by subtracting a sky gradient computed by fiting with a 2D polynomial of level two from the image after masking any bright source. This removes fluctuations and flux contamination from neighbouring galaxies, what we found was helpful to reduce the uncertainties in the faint areas for some galaxies in the samples like NGC 1042. To create a mask, the package *segmentation* from *photutils* (Bradley et al. 2024) is used. A binning of (13x13) pixels is applied on the masked images to increase the SNR. This value of this binning is chosen according to the binning applied by Pohlen & Trujillo (2006) with SDSS data in their study aiming to characterize the structure of disks and the different types of truncation in the surface brightness profiles. Faint artifacts and objects appearing in the binned images are then masked. A first set of ellipses is executed using *Ellipses* from photutils to determine the position angle and the ellipticity at the edges of the galaxies in a similar way to what Merritt et al. (2016) did on NGC1042 with Dragonfly data. Then a second set of ellipses is run with the position angle and the ellipticity (e) fixed with the values found above. The Table 1 gives the position angle (PA) and the ellipticity found for the three galaxies with this method.
In order to determine the errors, 24 boxes are created around the galaxies in which the mean (μ), the standard

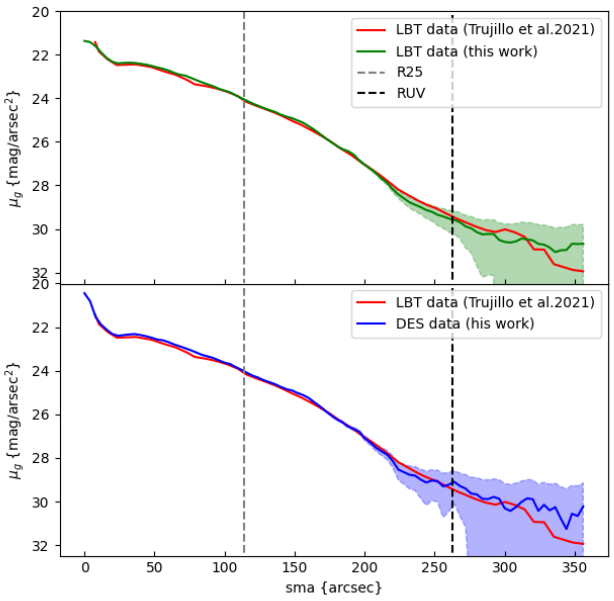

Fig. 2. Surface brightness profile in g-band for NGC1042 as a function of the semi-major axis of ellipses. **Top:** Profile from Trujillo et al. (2021) with LBT data (in red) compared to our method applied to the same data(in green) **Bottom:** Profile from Trujillo et al. (2021) with LBT data (in red) compared to our method applied to DES data (in blue). The grey dashed line is the R_{25} of the galaxy when the black dashed line is the R_{UV}.The shaded area shows the uncertainties for LBT data with the method used here in the top panel and DES data with the method used here in the bottom panel

.

deviation and number of pixels is calculated. Only the boxes with μ within five sigma of its average $< \mu >$ are retained to avoid boxes with unmasked bright stars or artefacts. Then errors on the surface brightness are computed as in Gil de Paz & Madore (2005) and the $< \mu >$ is subtracted from the profiles.

To ensure that the depth of the DES data is sufficient and that our method is robust, we first utilized this method with the LBT data in comparison with the profile obtained by Trujillo et al. (2021) with the same data. The two profiles shown in the top panel of the Fig. 2 are similar. The surface brightness obtained following our method is well consistent with the one published by Trujillo et al. (2021) when using the same data. The bottom panel compares the profile of Trujillo et al. (2021) with LBT data with the method used in this study with DES data. This allows us to establish that DES data are adequate to study the XUV galaxies in their extended UV regions. The errors bars are smaller in the profile with LBT data than with the DES data, for which the data are more noisy. Then we used the same method to calculate the FUV and NUV profiles of GALEX. The FUV and NUV images are projected on the DES pixels.

In the previous figure, we used R_{UV} to define the end of the XUV region. While the R_{UV} is often defined as the last galaxy radius with useful UV data (Gil de Paz et al. 2007; Boissier et al. 2008), we define a physically motivated systematic R_{UV} as follows. We started by calculating the star formation ratio surface density Σ_{SFR} in the FUV band of GALEX taking into account the inclination correction and using theUV-SFR calibration

Name	R.A. (degrees)	Dec. (degrees)	R_{25} (arcsec)	PA (degrees)	e	R_{UV} (arcsec)
NGC1042	40.099863	-8.433544	114	71	0.17	239
NGC0991	38.886187	-7.154435	48	68	0.11	152
NGC1051	40.260372	-6.935918	54	139	0.37	163

Table 1. Properties of the sample. R.A. and Dec. come from NED, the R_{25} from Thilker et al. (2007), PA, e and R_{UV} from this study

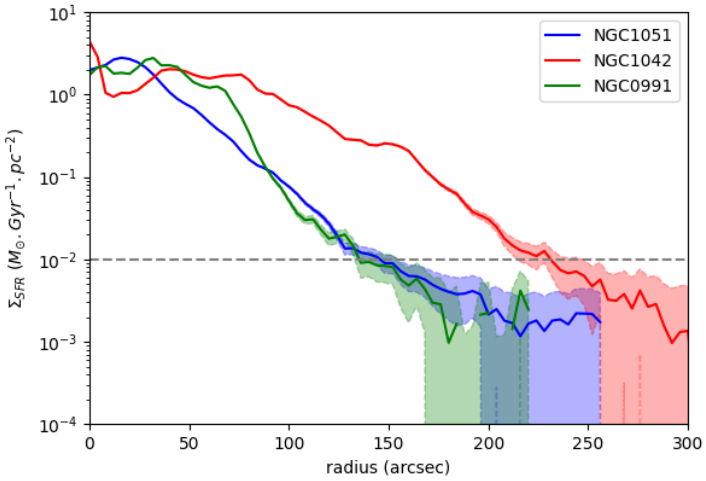

Fig. 3. Star Formation Rate Surface Density (Σ_{SFR}) as a function of the radius estimated using the GALEX FUV data of the sample

of Boissier (2013) with the IMF by Kroupa (2001). Then the UV radius is chosen for a constant value of $\Sigma_{SFR} = 10^{-2}\ M_\odot.Gyr^{-1}.pc^{-2}$, shown in Fig 3. This value was based on the outer radii of the profiles of nearby galaxies studied in Bigiel et al. (2008) and Malin 1 in Junais et al. (2024). This value was chosen because of its simplicity and the fact that it is well consistent with the largest star-forming regions seen in such galaxies. The R_{UV} calculated for each galaxy in the sample is given in the Table 1.

2.2 Results

We separate the profiles in two regions: the inner part and the XUV regions from R_{25} to R_{UV} and apply an exponential fitting for each part. This is a very basic procedure that allows a universal easy to implement method. If the profiles are not perfectly fit, it still gives a good order of magnitude of the extent and surface brightness of each regions. We obtain two set of values for each galaxies shown in Fig. 1. The three galaxies are LSB for the inner region. For the XUV part, we observe two different behaviors: One galaxy of the sample (NGC1051) has both its XUV region and inner disk in the LSB part of the figure while the two others have their XUV disks in the HSB area. It seems to come from the morphology of the profiles and their type. For the galaxy with both regions in the LSB area, the profile is antitruncated while the profile of the two others are truncated (as defined in Pohlen & Trujillo 2006).

3 Conclusions

The first steps described in these proceeding show that we can use deep images like the one provided by the DES survey to characterize the optical properties of XUV galaxies in their extended UV region. The first three galaxies we studied are about one magnitude below the Freeman (1970) value when looking the inner region. In the extended regions, this is not the case for each galaxies in the sample and it shows a more complex behavior. The future steps for this study are to analyse the complete sample, compare those galaxies with Malin 1 (treated in the same way), analyze the color profiles. They will be presented in Bernaud et al., in preparation. It is also an example of application for the future telescope CASTLE in construction at Calar Alto, for which the LSB galaxies are one of the main science case, thanks to it innovative design (Lombardo et al. 2020).

References

Abbott, T. M. C., Adamów, M., Aguena, M., et al. 2021, The Astrophysical Journal Supplement Series, 255, 20

Bigiel, F., Leroy, A., Walter, F., et al. 2008, The Astronomical Journal, 136, 2846–2871

Boissier, S. 2013, in Planets, Stars and Stellar Systems. Volume 6: Extragalactic Astronomy and Cosmology, ed. T. D. Oswalt & W. C. Keel, Vol. 6, 141

Boissier, S., Gil de Paz, A., Boselli, A., et al. 2008, The Astrophysical Journal, 681, 244–257

Bradley, L., Sipőcz, B., Robitaille, T., et al. 2024, astropy/photutils: 1.12.0

Freeman, K. C. 1970, ApJ, 160, 811

Gil de Paz, A., Boissier, S., Madore, B. F., et al. 2007, ApJS, 173, 185

Gil de Paz, A. & Madore, B. F. 2005, The Astrophysical Journal Supplement Series, 156, 345

Hagen, L. M. Z., Seibert, M., Hagen, A., et al. 2016, The Astrophysical Journal, 826, 210

Junais, Weilbacher, P. M., Epinat, B., et al. 2024, Astronomy & amp; Astrophysics, 681, A100

Kroupa, P. 2001, MNRAS, 322, 231

Lombardo, S., Prada, F., Hugot, E., et al. 2020, CASTLE: performances and science cases

Merritt, A., Dokkum, P. v., Abraham, R., & Zhang, J. 2016, The Astrophysical Journal, 830, 62

Pohlen, M. & Trujillo, I. 2006, Astronomy & amp; Astrophysics, 454, 759–772

Sprayberry, D., Impey, C. D., Bothun, G. D., & Irwin, M. J. 1995, AJ, 109, 558

Thilker, D. A., Bianchi, L., Meurer, G., et al. 2007, The Astrophysical Journal Supplement Series, 173, 538–571

Trujillo, I., D'Onofrio, M., Zaritsky, D., et al. 2021, Astronomy & amp; Astrophysics, 654, A40